Swept Wing Ice Accretion Modeling

M.G. Potapczuk
C.S. Bidwell
National Aeronautics and Space Administration
Lewis Research Center
Cleveland, Ohio 44135

SUMMARY

An effort to develop a three-dimensional ice accretion modeling method has been initiated. This first step towards creation of a complete aircraft icing simulation code builds on previously developed methods for calculating three-dimensional flowfields and particle trajectories combined with a two-dimensional ice accretion calculation along coordinate locations corresponding to streamlines. This work is intended as a demonstration of the types of calculations necessary to predict a three-dimensional ice accretion. Results of calculations using the 3D method for a MS-317 swept wing geometry are projected onto a 2D plane normal to the wing leading edge and compared to 2D results for the same geometry. It is anticipated that many modifications will be made to this approach, however this effort will lay the groundwork for future modeling efforts. Results indicate that the flowfield over the surface and the particle trajectories differed for the two calculations. This led to lower collection efficiencies, convective heat transfer coefficients, freezing fractions, and ultimately ice accumulation for the 3D calculation.

NOMENCLATURE

A	=	area for convection heat transfer	h, HTC	=	convective heat transfer coefficient
A_m	=	area that particles impact on the surface	i, j	=	grid indices
A_o	=	area through which a group of particles travel at release plane	L_v	=	latent heat of vaporization
C_p	=	pressure coefficient	$\dot{m}_c$	=	mass flux determined from collection efficiency values
C_{p_w}	=	specific heat of water	$\dot{m}_e$	=	mass flux evaporating from the surface
d_{ice}	=	ice thickness	$\dot{m}_i$	=	mass flux freezing
f, FF	=	freezing fraction			

$\dot{m}_{r_{in}}$	=	runback mass flux from the previous control volume	T_S, TS	=	temperature at the surface
$\dot{m}_{r_{out}}$	=	mass flux into the downstream control volume	T_∞	=	temperature in the free stream
$\dot{q}_c$	=	heat flux due to the impacting water droplets	t	=	time
$\dot{q}_{cond}$	=	heat flux due to conduction through the ice/airfoil surface	u	=	weighting factor in j-direction
$\dot{q}_{conv}$	=	heat flux due to convection	VE	=	local inviscid velocity
$\dot{q}_{evap}$	=	heat flux due to evaporation	V_∞	=	free-stream velocity
$\dot{q}_i$	=	heat flux required for phase change of water to ice	v	=	weighting factor in i-direction
$\dot{q}_{r_{in}}$	=	heat flux associated with the incoming runback water	W	=	unit width
$\dot{q}_{r_{out}}$	=	heat flux associated with the outgoing runback water	$\vec{X}_i$	=	displacement vector from x(i,j) to x(i+1,j)
Re	=	Reynolds number	$\vec{X}_j$	=	displacement vector from x(i,j) to x(i,j+1)
S	=	surface	$\vec{X}_s$	=	displacement vector from x(i,j) to x_s
s	=	surface distance	x_s	=	location along surface streamline
			x_c	=	location of centroid of A_m
			β,BETA	=	collection efficiency
			γ	=	sweep angle
			ρ	=	density

I. Introduction

Ice accretion modeling has received considerable attention during the past few years. The National Aircraft Icing Technology Plan[1], drafted in 1986 under the direction of several federal agencies, calls for the creation of a complete aircraft icing simulation during the coming decade. In support of this plan several activities related to the creation of a 2D ice accretion modeling and performance evaluation capability have been undertaken at the NASA Lewis Research Center. A 2D ice accretion code, LEWICE, was developed in 1983 by the University of Dayton Research Institute[2] and later modified by Ruff[3]. This code is divided into three major parts; a potential flow calculation, a particle trajectory calculation, and an ice growth calculation. The ability of LEWICE to predict airfoil ice accretions is quite good for rime ice growths. Glaze ice predictions, although acceptable, have exhibited some deficiencies which have been documented by several authors[4-6]. The calculation of performance degradation due to icing is an equally important aspect of the icing analysis problem. Over the past several years 2D calculations for iced airfoils have been performed using the interactive boundary layer method[7] and using Navier-Stokes codes[8]. Recently, Cebeci[9] has combined his interactive boundary layer method with LEWICE. This has resulted in a code which has the potential to accurately determine the flowfield and particle trajectories while also providing the performance degradation information during a single calculation.

With these activities firmly underway, it is appropriate to consider the methodology for development of a three-dimensional ice accretion analysis capability. Some of the issues associated with a 3D icing calculation are the same as those for 2D. On the other hand, some issues only become evident when considering a full 3D calculation. These may include; variations in ice growth on both a large and small scale across a wing span, runback in the spanwise direction, non-uniformities in the impinging cloud along the span, and particle trajectories in complex geometric regions.

The current effort is directed at taking existing computer codes and developing a strategy for performing a 3D ice accretion and performance degradation calculation for a swept wing configuration. This activity will serve as a demonstration calculation and as a focus for future development of the approach. The computer codes used in this effort consist of a 3D panel code, a particle trajectory code, and the ice accretion subroutines of the LEWICE code. The performance calculations will use a 3D Navier-Stokes code, ARC3D. Presently, the calculations are performed separately. In the future, these calculations will be performed in a single code thus requiring less user interaction than is currently necessary. This report describes the ice accretion calculation as applied to an infinite swept wing configuration.

The wing geometry chosen for this calculation is that of an MS-317 airfoil with a 30° sweep angle, as shown in Figure 1. The MS-317 airfoil model represents a typical medium-speed wing section. This geometry was chosen due to the availability of experimental information from ice accretion tests currently being carried out in the NASA Lewis Icing Research Tunnel. Comparisons of the predicted ice accretion profiles to those of the experiment will be completed as a follow-on to this work.

II. Code Description

A 3D ice accretion calculation for a complete aircraft is a major step forward from current capabilities. The present activity is directed at extending current 2D capabilities to simple 3D geometries by assuming constant spanwise gradients. For this work, an infinite swept wing of constant geometry in the spanwise direction is used. Such a geometry produces similar streamlines along the span. As a result of this streamline similarity, it is assumed that there is no net transport of water across the control volume in the spanwise direction. The control volume analysis of the ice accretion can thus be considered two dimensional and the 2D LEWICE routines can be used. This also allows a single evaluation of the ice growth for any streamline to represent the ice accretion behavior for any location on the wing. Since the resulting ice shape geometry will not vary along the span, re-paneling of the iced wing for subsequent ice accretion calculations is simplified.

An infinite swept wing also avoids consideration of ice growth near the tip of the wing or at the wing-body junction. At these locations, the flowfield is quite irregular and major changes to the approach currently being employed would be required. It is anticipated that future work in 3D ice accretion prediction would be directed at addressing these regions of the flowfield. Currently, the tools

necessary for evaluation of these complex flowfields are being developed by Sankar[10] and Caruso[11]. Additional work will be required to create a 3D control volume analysis for the ice accretion calculation. As these codes become available, they will be incorporated into the 3D ice accretion analysis methodology.

II-1. 3D Panel Code and Particle Trajectory Calculation

The flowfield and particle trajectory calculations are extensions of the 2D analysis methods used in LEWICE. The three-dimensional flowfield calculation uses a Hess-Smith panel code[12]. The code can accomodate lifting and non-lifting geometries or combinations, thus allowing simulation of complex surfaces such as a complete aircraft (Figure 2). A Prandtl-Glauert correction is used to allow compressible flow calculations. The code can also handle leaking panels to simulate inlets or instrument orifices. The code provides velocity information at any point in the flowfield away from the surface. This type of code uses very little computer time compared to a viscous flow code and yet provides sufficient flowfield information for subsequent trajectory and energy balance calculations under most circumstances.

The trajectory calculation is based on the computer code developed by Norment[13] with one additional feature. The code solves a force balance equation on a single particle and then determines the new particle position using an Adams-type predictor-corrector algorithm developed by Krogh[14]. The added feature is the ability to calculate the local collection efficiency from the impacting particles. The code generates an array of impingement points for each region of interest. This is done by releasing an array of particles which impact the region of interest (Figure 3). The collection efficiency is the ratio of the particle flux at the target point to the free-stream particle flux. If a known group of particles is tracked from their release location to the target location, then the collection efficiency can be determined by the ratio of the target area to the release area. The collection efficiency can then be determined from the following relationship,

$$\beta(x_c(i,j)) = A_o(i,j)/A_m(i,j) \tag{1}$$

Once the collection efficiency is determined for the surface, an array of surface locations and corresponding β values is created for streamlines on the surface. This information will be used in the ice accretion calculation to determine ice growth along the streamline paths. The streamlines are calculated using a 4th order Runge-Kutta integration scheme. The streamline is carried forward from the stagnation region for both the upper and lower surface at the region of interest.

A linear interpolation scheme is used to determine the collection efficiency along the streamline from the matrix of β values generated in the trajectory calculation. The array of β values is searched to find the surface cell in which the streamline point resides (Figure 4). The β value at the streamline

point is then determined from a weighted average of the local collection efficiencies at the four surrounding cell points. The interpolation expression is,

$$\beta(x_s) \simeq \beta\Big(x_c(i+1,j+1)\Big)\cdot u\cdot v + \beta\Big(x_c(i,j+1)\Big)\cdot u\cdot(1-v) + \beta\Big(x_c(i,j)\Big)\cdot(1-u)\cdot(1-v) + \beta\Big(x_c(i+1,j)\Big)\cdot(1-u)\cdot v \tag{2}$$

where,

$$u = \vec{X}_s \cdot \vec{X}_j \tag{3}$$

and

$$v = \vec{X}_s \cdot \vec{X}_i \tag{4}$$

represent weighting factors in the interpolation based on the geometry of the cell.

II-2. Ice Accretion Calculation

The ice accretion calculation is performed as a 2D strip analysis along streamlines calculated by the 3D panel code. The results of the previous calculation are written into a file containing the x,y,z coordinates of the streamline, the surface distance between points, the x,y,z components of the unit normal vector for the panel at the streamline coordinate locations, the velocities, and the local collection efficiencies, β. The subroutines from the LEWICE code which determine the boundary layer values, the control volume energy balance and the resulting ice growth are used to determine the ice shape at a given spanwise location. A brief outline of the LEWICE calculation follows. Further details can be found in reference 3.

The ice accretion calculation consists of a control volume mass and energy balance. The 2D strip analysis allows use of the assumption that there are no spanwise fluxes into the control volume, which is consistant with the infinite swept wing flowfield assumption. A depiction of the control volume for the process is shown in Figure 5. The Δs value is based on distance along the streamline.

The mass balance equation is,

$$\dot{m}_c + \dot{m}_{r_{in}} = \dot{m}_e + \dot{m}_{r_{out}} + \dot{m}_i \tag{5}$$

The impinging mass flux, $\dot{m}_c$, is determined from the β distribution. The mass flux into the control volume, $\dot{m}_{r_{in}}$, is any water remaining in the liquid state after evaluation of an upstream control volume. This mass flux is called runback. The mass flux out of the control volume due to evaporation, $\dot{m}_e$, and to freezing, $\dot{m}_i$, are determined from the energy balance calculations. The mass flux out of the control volume, $\dot{m}_{r_{out}}$, is used as input for the downstream control volume. The

freezing fraction is a term used to describe the fraction of incoming liquid that freezes within the control volume. It is given by the expression,

$$f = \frac{\dot{m}_i}{\dot{m}_c + \dot{m}_{r_{in}}} \tag{6}$$

The energy balance equation is,

$$\dot{q}_c + \dot{q}_{r_{in}} = \dot{q}_{cond} + \dot{q}_{evap} + \dot{q}_{conv} + \dot{q}_{r_{out}} + \dot{q}_i \tag{7}$$

The values of $\dot{q}_c$ and $\dot{q}_{r_{in}}$ are obtained from mass flux values and the internal energy levels of the incoming water. Integral boundary layer expressions are used to determine the heat flux due to convection. The inviscid flowfield values are used as boundary values for the viscous calculation. The boundary layer calculation determines the location of transition from laminar to turbulent flow and then uses an appropriate value of the convection heat transfer coefficient. The heat transfer value is then obtained by use of Newton's law of cooling,

$$\dot{q}_{conv} = h\, A \left(T_s - T_\infty\right) \tag{8}$$

The evaporative heat flux is also obtained from consideration of the inviscid flowfield conditions using the expression,

$$\dot{q}_{evap} = \dot{m}_e \left(C_{p_{w,s}} T_s + L_v\right) \Delta s \tag{9}$$

where the evaporative mass transfer rate, $\dot{m}_e$, is determined from local pressure and temperature conditions. Further details on this calculation are found in reference 3. The heat flux due to conduction is a user specified value. This leaves two equations for the two unknowns, $\dot{m}_{r_{out}}$ and $\dot{m}_i$.

The mass of ice that freezes is used to determine the thickness of the resulting ice layer. Since the analysis is locally 2D, the ice thickness can be found from the relation,

$$d_{ice} = \frac{\dot{m}_i \Delta t}{\rho_{ice}\ \Delta s\ W} \tag{10}$$

The thickness is then considered to be uniform over the entire panel for subsequent flowfield calculations. The new coordinates for the panel are obtained from the relation,

$$x_i = x_i + d_{ice}\, \hat{x}_i \tag{11}$$

where x_i is the ith coordinate of the center of the panel and $\hat{x}_i$ is the ith component of the unit normal vector for the panel.

As the ice thickness increases, there is the possibility that ice segments will intersect and thus this must be accounted for in the determination of the new geometry. Since this is a strip analysis, the spanwise thickness does not vary. Therefore, the possibility of ice growth intersection is limited to the normal and chordwise directions. In that case, the line segments corresponding to the top of every other panel are examined for intersection. If intersection is determined to occur, then a new panel is formed with its center halfway between the two old panels. This requires determination of the coordinates of the new panel and renumbering of the panels. This information is then used in subsequent potential flow calculations.

III. Results and Discussion

Prior to the development of modern computational techniques, Dorsch and Brun[15] devised a method for determining cloud-droplet impingement on swept wings. Their approach is based on the argument that droplet trajectories for an infinite swept wing can be calculated in the same manner as for a 2D plane normal to the leading edge of the wing, using the component of the free-stream velocity in that plane. Thus, the impingement limits, local collection efficiencies, and total water collected are calculated for the normal plane. The results are then considered to be equivalent at all normal planes along the span.

An examination of that approach can be undertaken by comparing results of the current method to a 2D LEWICE calculation for a normal plane of the swept wing configuration. In order to compare the swept to unswept condition, the approach velocity of the 2D calculation was taken as the component of the swept wing velocity in the normal plane. If γ is the sweep angle, then the appropriate 2D approach velocity is found using the relation,

$$V_{\infty_u} = V_{\infty_s} \cos \gamma \tag{12}$$

In order to understand the forces exerted on the incoming particles, it is illustrative to compare the relative strengths of the pressure fields for the two cases to the inertia of the incoming water droplets. The inertia of the droplets is characterized by the expression,

$$\tfrac{1}{2}\rho_w V_\infty{}^2 \tag{13}$$

An alternate pressure coefficient based on the droplet inertia would have the form,

$$\hat{C}_p = \frac{p - p_\infty}{\tfrac{1}{2}\rho_w V_\infty{}^2} \tag{14}$$

This term is simply related to the standard pressure coefficient through the ratio of water to air densities. Thus, the standard C_p values based on the density of air and the approach velocity can be used to evaluate the forces exerted on the water droplets. These are plotted in Figure 6 for the two cases considered.

The 3D potential flow calculation for the MS-317 wing section with a 30° sweep angle yielded pressure coefficient profiles in a plane normal to the leading edge as shown in Figure 6. The C_p distribution is contrasted to that of a 2D airfoil section in the figure to show the influence of the sweep angle. The swept wing C_p distribution has somewhat higher pressure values on the suction surface. Based on the discussion above, this indicates that the swept wing suction pressure has less influence on the incoming particle trajectories than the 2D suction pressure. This difference causes a shifting of the local collection efficiency distribution, as discussed below. The differences in flowfield characteristics also have an impact on the convective heat transfer in the region of ice accretion.

Three-dimensional particle trajectory calculations from this flowfield are shown in Figure 7. The trajectories indicate particle motion in the spanwise direction in the region just in front of the wing. Apparently the influence of the spanwise velocities is not felt until the particles are close to the surface. The free-stream velocity, sweep angle, and particle size all play a role in the extent of spanwise travel. The particles thus impact the surface at some angle with respect to the chordwise direction. The effect of this 3D particle trajectory is evident in the local collection efficiency plots, as shown in Figure 8. Additionally, more complex geometries would affect particle trajectories to a greater degree than the simple geometry examined here.

Along the streamline, the local collection efficiencies are determined according to Eq. 2. For comparison purposes, a plot of β vs. distance from the stagnation point in a plane normal to the leading edge of the wing, along with 2D results for the same geometry, are shown in Figure 8. The 3D β curve has impingement limits at a distance somewhat closer to the stagnation point than the 2D case. Additionally, the 3D results indicate a somewhat lower β near the stagnation region. This behavior is most noticeable for the suction surface (i.e. positive s values). The higher pressure levels on the suction surface of the 3D calculation result in a relative shift of the particle trajectories to the pressure surface compared to the 2D case. This combined with spanwise motion of the particles described above account for the different β distributions.

The convective heat flux term has a major influence on the control volume energy balance. The velocity distribution over the surface and the resulting convective heat transfer coefficient are shown in Figures 9 and 10 respectively. Since the spanwise velocity does play a role in the convective heat transfer of the energy balance, the total free-stream velocity was used in this portion of the 2D calculation. The velocity distributions are somewhat different for the two calculations. The higher pressure of the 3D calculation is reflected in the lower velocity levels. This results in lower heat transfer coefficient values for that surface. The greatest differences are in the stagnation region. The

milder pressure-side inviscid velocity gradients from the 3D calculation result in a lower heat transfer coefficient value. This suggests the possibility of more runback water on the pressure side for the 3D calculation. Additionally, the 2D calculation produces smoother distributions. Examination of interpolation routines and surface panel distribution is required.

These changes in the heat transfer distribution on the surface combined with the altered β distribution lead to differences in the surface temperature and freezing fraction, as shown in Figures 11 and 12 respectively. Both figures show the shifting of the region of ice accumulation to the pressure side of the wing. The surface temperature plots show a small region of transition from an ice/water interface (indicated by the regions where T is constant at 0°C) to a completely dry, iced surface (indicated by the regions where T is constant at approximately -16°C) for the 2D calculation. The 3D calculation indicates a dry iced surface over the entire accretion area. The large gradient in surface temperature at s = 0.024 for the 3D calculation may be due to the sharp spikes in the heat transfer coefficient distribution. The freezing fraction plots indicate a small region of wet ice growth for the 2D calculation and a completely dry ice growth for the 3D calculation. The heat transfer coefficient in this region does not drop as low for the 3D calculation as it does in the 2D calculation. This results in sufficient energy loss to provide for freezing of all the incoming water.

The ice accretion results for this wing are shown in Figure 13. Comparison to the 2D results indicate the influence of the altered collection efficiency distribution and of the 3D flowfield. The ice shape obtained with the 3D calculation has less mass and extends over a smaller portion of the surface. In this calculation, that shape would then be considered to be uniform along the span.

IV. Conclusion

An approach to calculate the ice accretion for an infinitely swept wing has been proposed. This method employs existing technology to couple the evaluation of 3D particle trajectories with a 2D strip analysis to predict ice buildup along surface streamlines. This reduces the computational resources that would be required for predicting the full 3D flowfield and uses only a small increase in resources over the current 2D LEWICE code. This approach could be easily extended to other simple 3D geometries such as axisymmetric engine inlets or rotor blades.

Comparisons to a 2D analysis were made for a MS-317 infinite swept wing geometry. Results indicate that the flowfield over the surface and the particle trajectories differed for the two calculations. This led to lower collection efficiencies, convective heat transfer coefficients, freezing fractions, and ultimately ice accumulation for the 3D calculation. These results also indicate that improvements can be made to the previously used method for evaluation of swept wing cloud-droplet impingement. The present calculations include the influence of sweep on pressure levels relative to droplet inertia.

Additional work is required to determine the number of panels necessary to accurately model the flowfield and resulting collection efficiency distribution for the swept wing. Studies of several swept

wing geometries are necessary to confirm the current results. Comparison to actual ice accretions for a swept wing geometry are also required to provide confidence in the calculation procedure. Future studies of the effects of finite span and wing/body junctions will be incorporated to give a prediction of the ice accretion distribution on complete wing geometries.

REFERENCES

1. National Aircraft Icing Technology Plan, Federal Coordinator for Meteorological Services and Supporting Services, Department of Commerce, FCM-P20-1986, April 1986.

2. MacArthur, C.D., Keller, J.L., and Leurs, J.K., "Mathematical Modeling of Ice Accretion on Aerofoils," AIAA-82-0284, 1982.

3. Ruff, G.A., "LEWICE : A User's Manual," To be published as a NASA CR in 1990.

4. Berkowitz, B.M. and Riley, J.T., "Analytical Ice Shape Predictions for Flight in Natural Icing Conditions," NASA CR-182234, 1989.

5. Hansman, R.J., Yamaguchi, K., Berkowitz, B., and Potapczuk, M.G., "Modeling of Surface Roughness Effects on Glaze Ice Accretion," AIAA Paper 89-0734, Jan. 1989.

6. Riley, J.T., "Uncertainty and Error Prpoagation in Aircraft Icing Calculations," AIAA Paper 90-0760, Jan. 1990.

7. Cebeci, T., "Prediction of Flow Over Airfoils with Leading Edge Ice," AIAA Paper 88-0112, Jan. 1988.

8. Potapczuk, M.G., "Navier-Stokes Analysis of Airfoils with Leading Edge Ice Accretions," PhD Dissertation, The University of Akron, May 1989.

9. Cebeci, T., Chen, H.H., and Alemdaroglu, N., "Fortified LEWICE with Viscous Effects," AIAA Paper 90-0754, Jan. 1990.

10. Sankar, L.N., "3D Performance Degradation Calculations for an Iced Wing," AIAA Paper 90-07XX, Jan. 1990.

11. Caruso, S.M., "Unstructured Grid Method for Viscous Flow Calculations of an Iced Airfoil," AIAA Paper 90-07XX, Jan, 1990.

12. Hess, J.L. and Smith, A.N.O., "Calculation of Potential Flow About Arbitrary Bodies," Progress in Aeronautical Sciences, Vol. 8, edited by D. Kuchemann, Pergammon Press, New York, 1967.

13. Norment, H.G., "Calculation of Water Drop Trajectories to and about Arbitrary Three-Dimensional Lifting and Nonlifting Bodies in Potential Airflow, NASA CR 3935, Oct. 1985.

14. Krogh, F.T., "Variable Order Integrators for Numerical Solutions of Ordinary Differential Equations," Jet Propulsion Lab Technology Utilization Document No. CP-2308, Nov. 1970.

15. Dorsch, R.G. and Brun, R.J., "A Method for Determining Cloud-Droplet Impingement on Swept Wings," NACA TN 2931, April 1953.

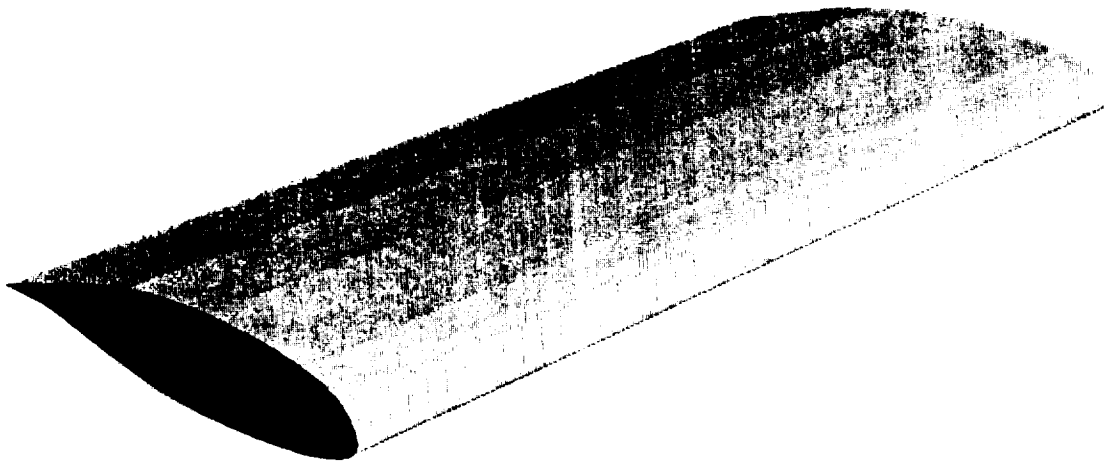

Figure 1 - MS-317 Swept Wing Profile

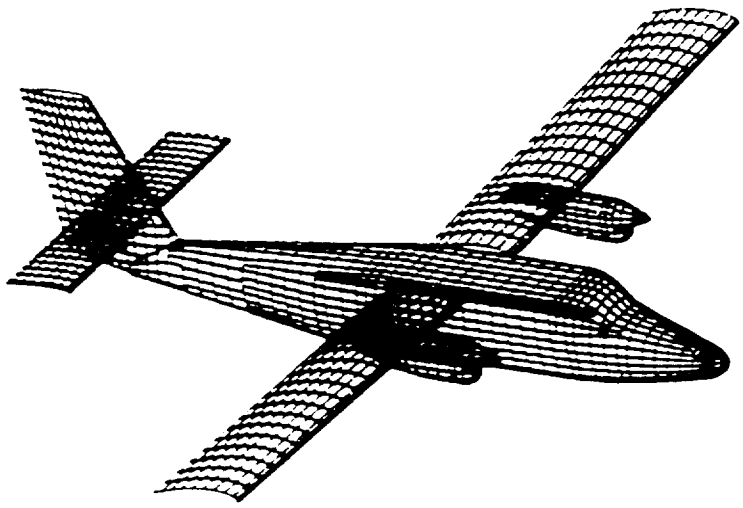

Finely resolved version

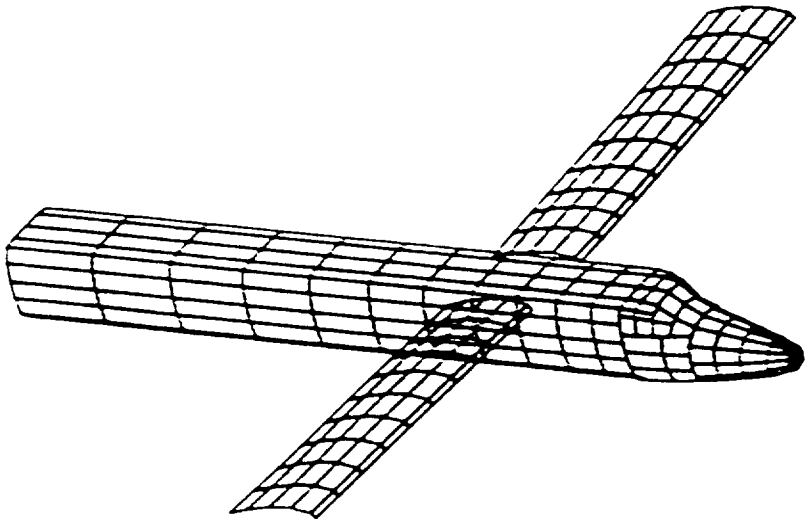

Coarsely resolved version

Figure 2 Digital description of the DeHavilland Twin Otter.

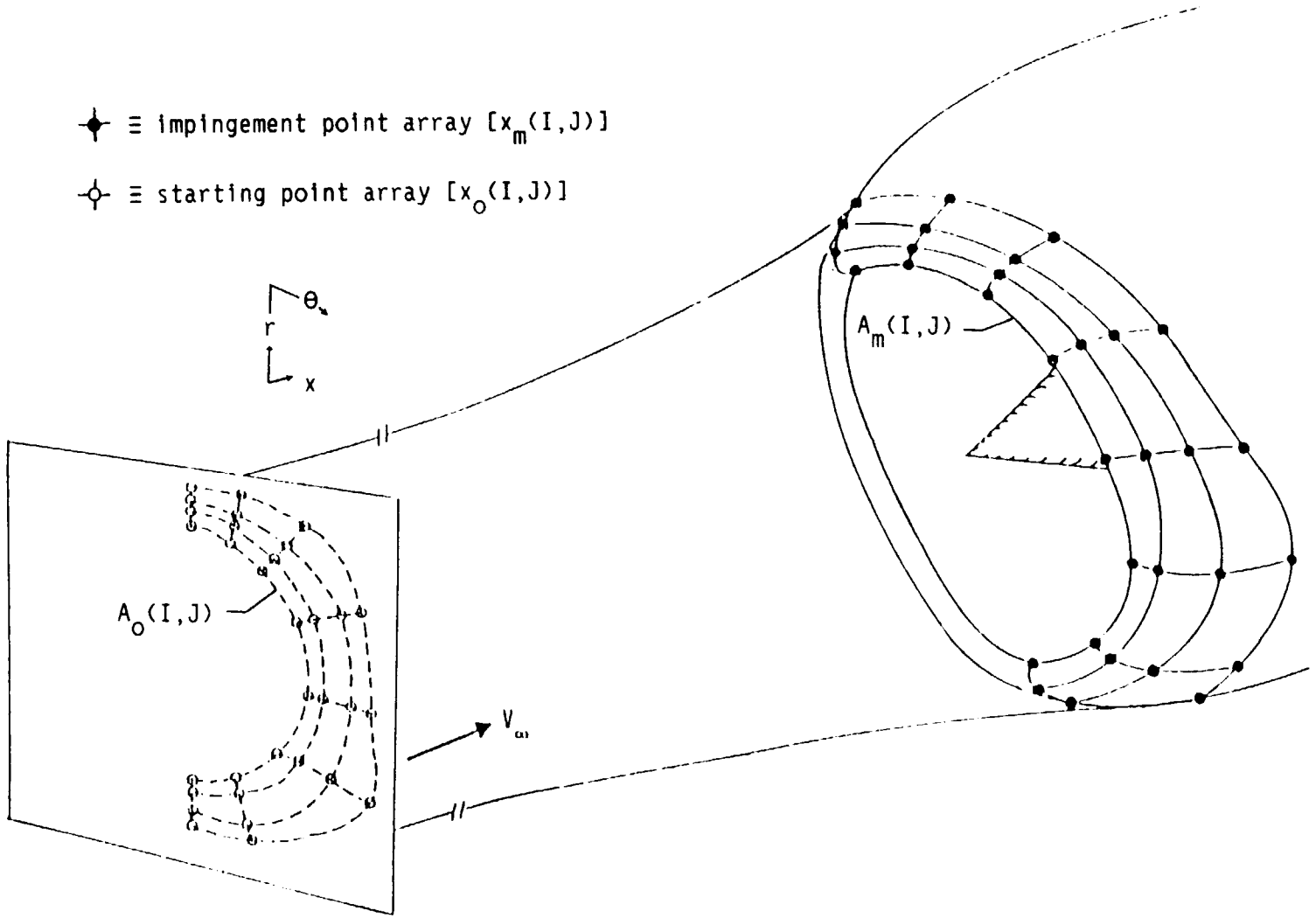

Figure 3 - Illustration of the Starting Point Array [$x_o(I,J)$] and Impingement Point Array [$x_m(I,J)$]

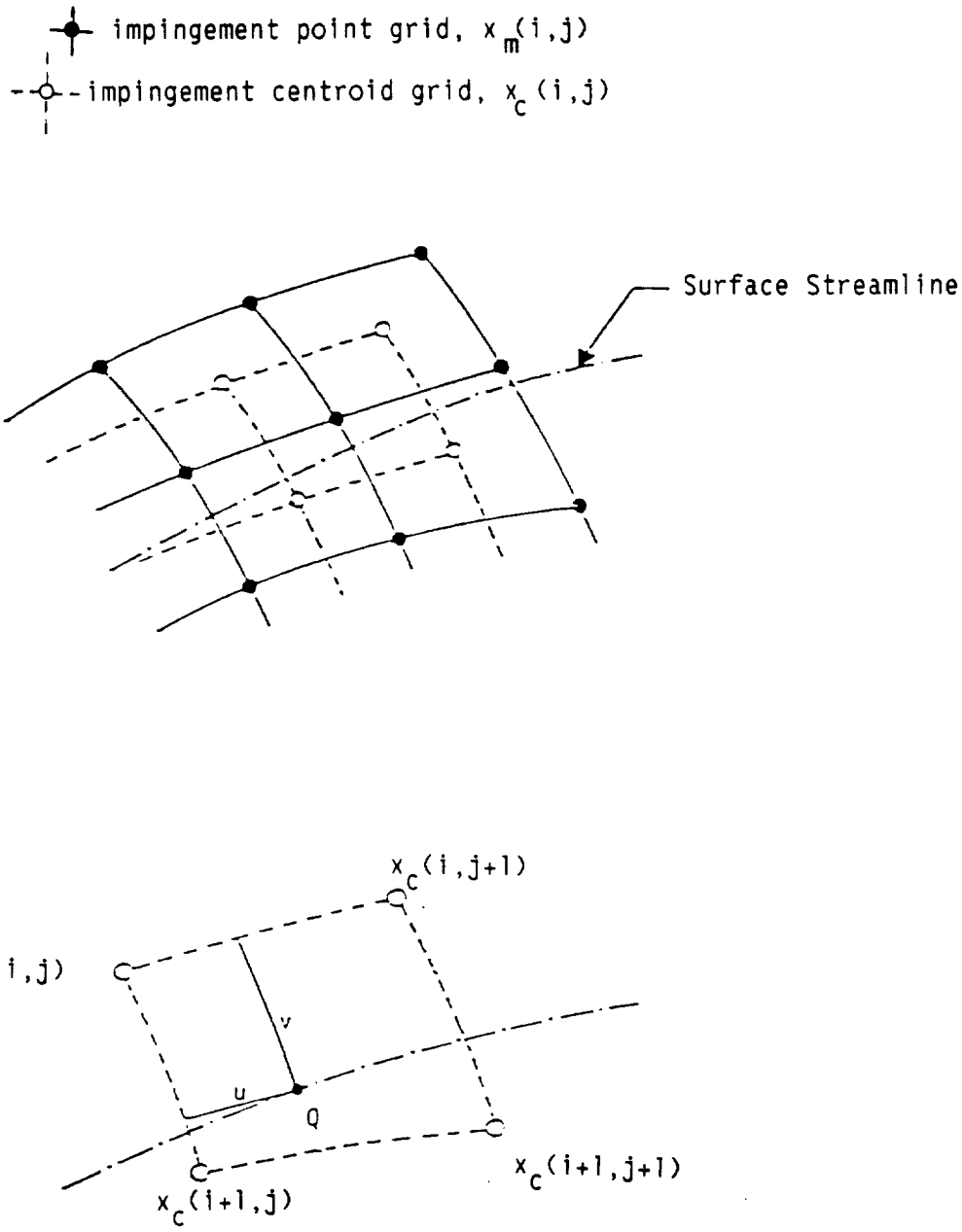

$$\beta(Q) \cong \beta(x_c(i+1,j+1))\cdot u\cdot v + \beta(x_c(i,j+1))\cdot u\cdot(1-v) + \beta(x_c(i,j))\cdot(1-u)\cdot(1-v)$$
$$+ \beta(x_c(i+1,j))\cdot(1-u)\cdot v$$

Figure 4 - Illustration of the Centroid Impingement Grid [$x_c(i,j)$] and β Interpolation

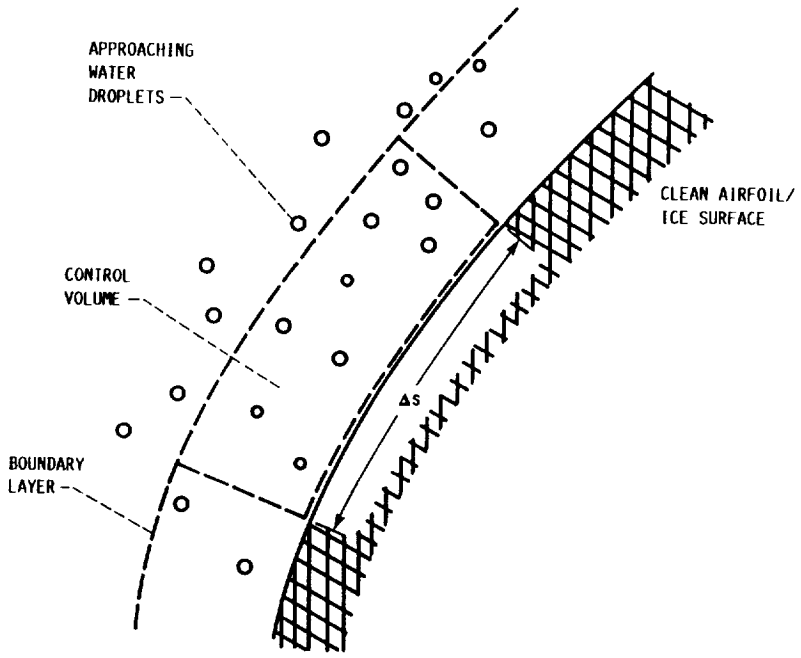

Figure 5. Control Volume for Ice Accretion Calculation

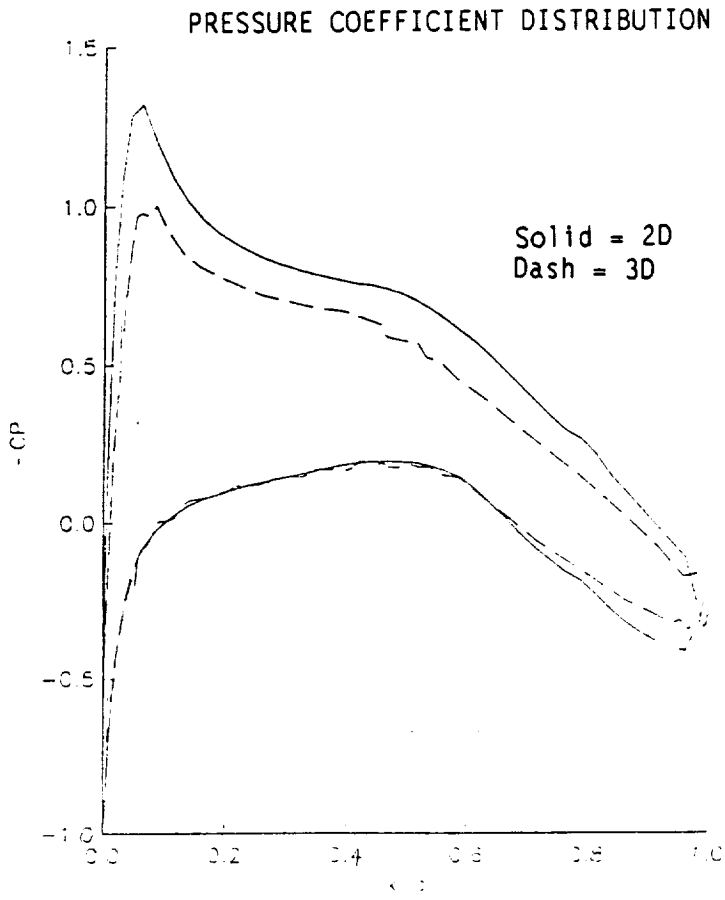

Figure 6 - Pressure Coefficient Distribution for MS-317 Profile: 2D and 3D Results

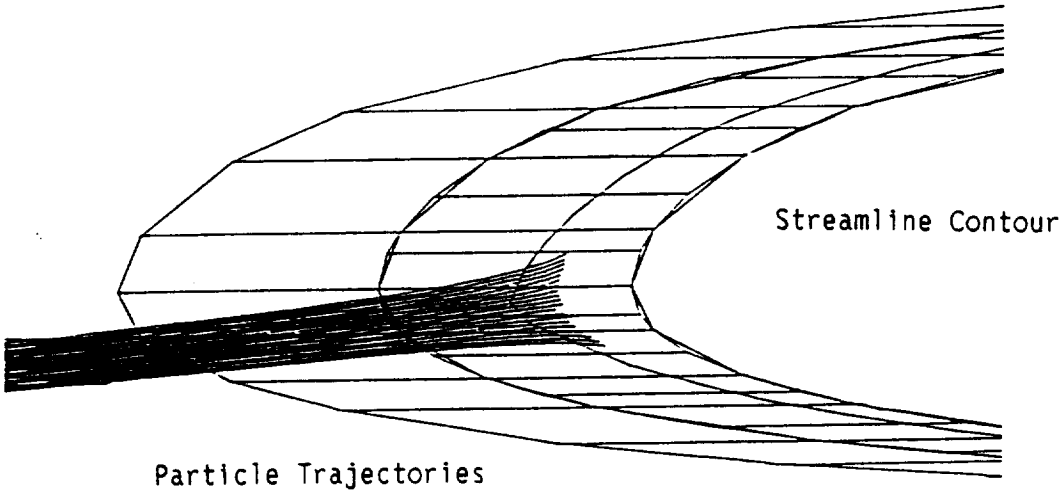

Figure 7 - Particle Trajectories and Streamline

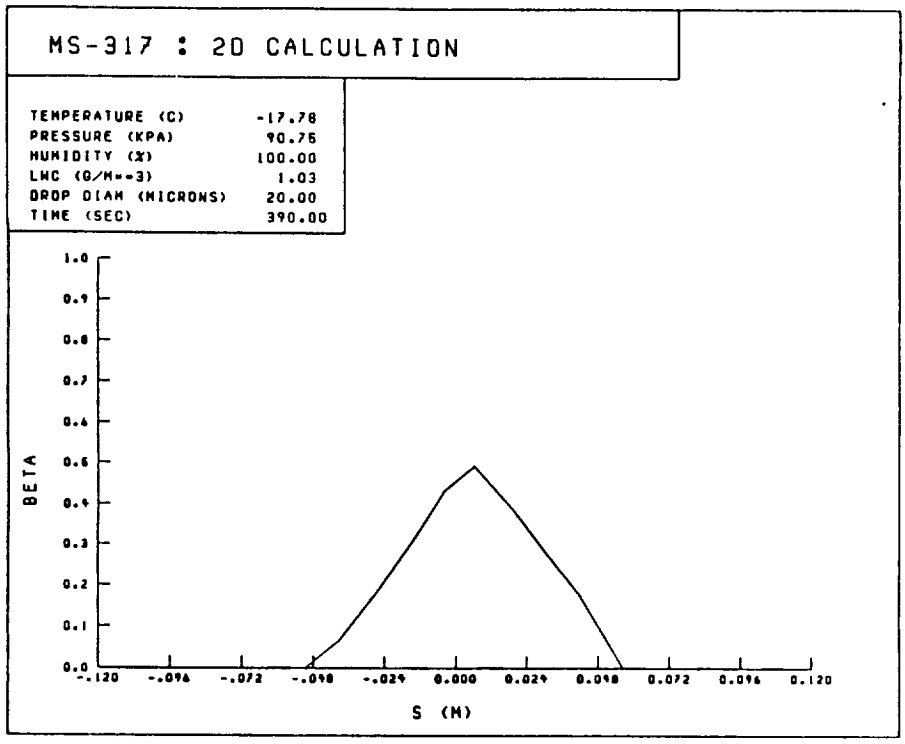

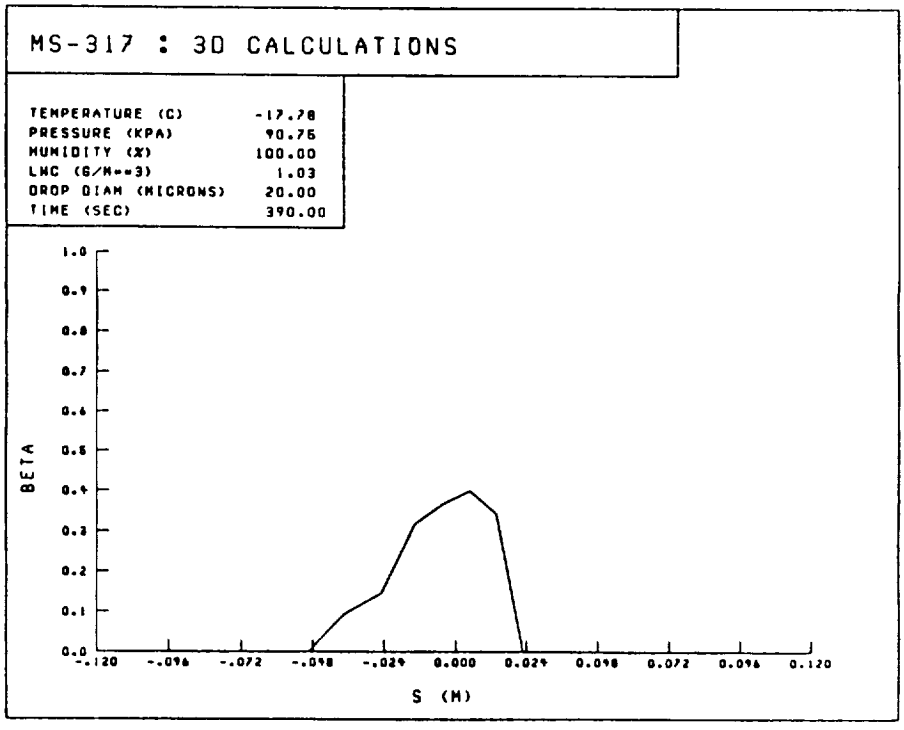

Figure 8. Local Collection Efficiency Distribution in a Plane Normal to the Leading Edge for a MS-317 Swept Wing ; 2D and 3D Calculations

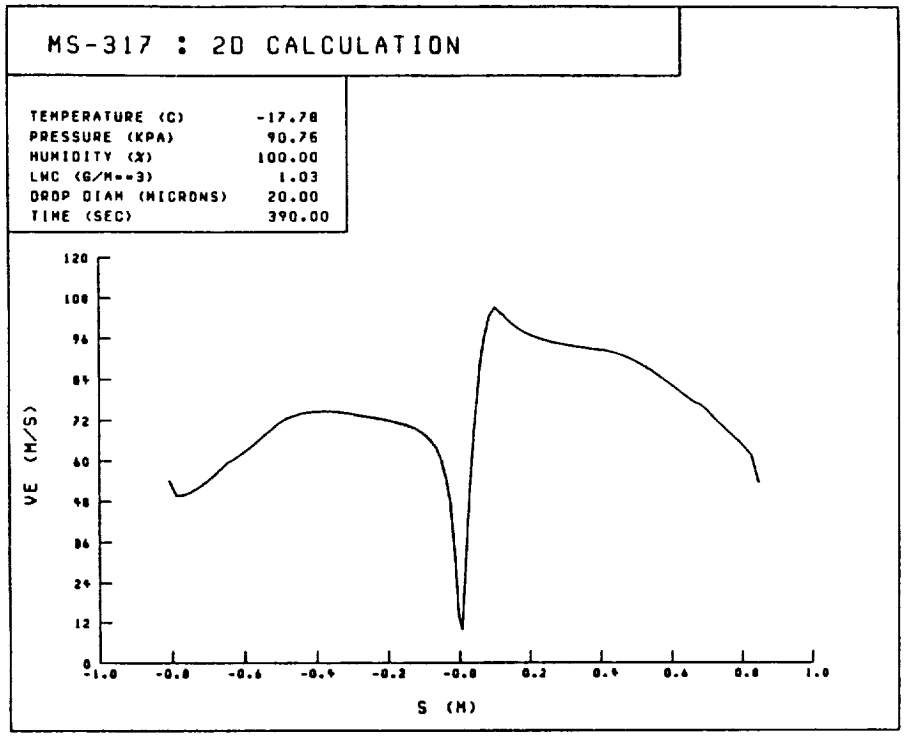

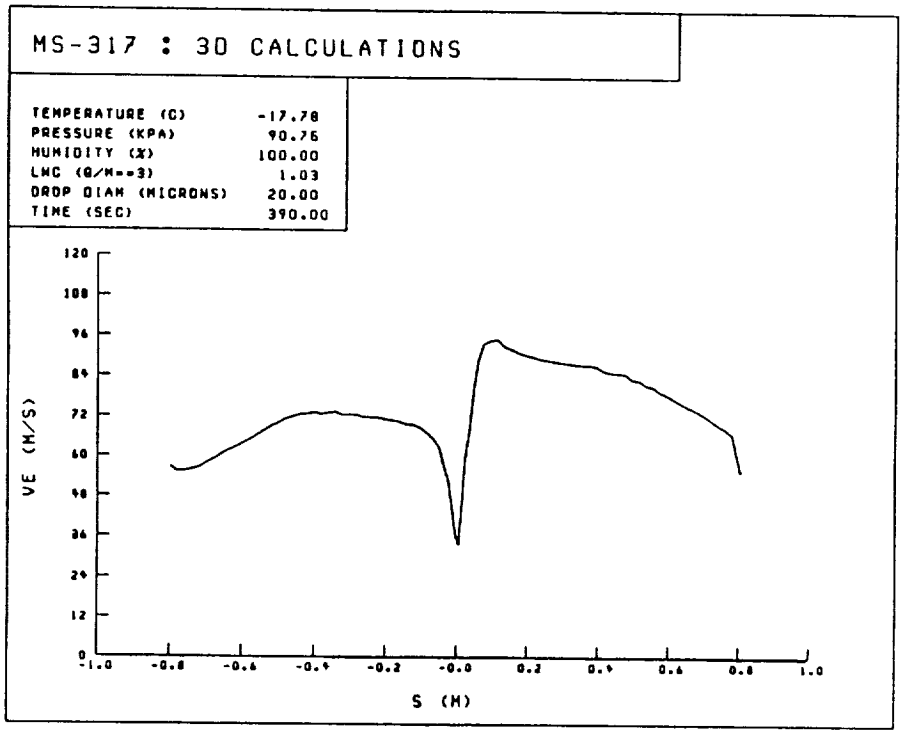

Figure 9. Local Inviscid Velocity Distribution in a Plane Normal to the Leading Edge for a MS-317 Swept Wing : 2D and 3D Calculations

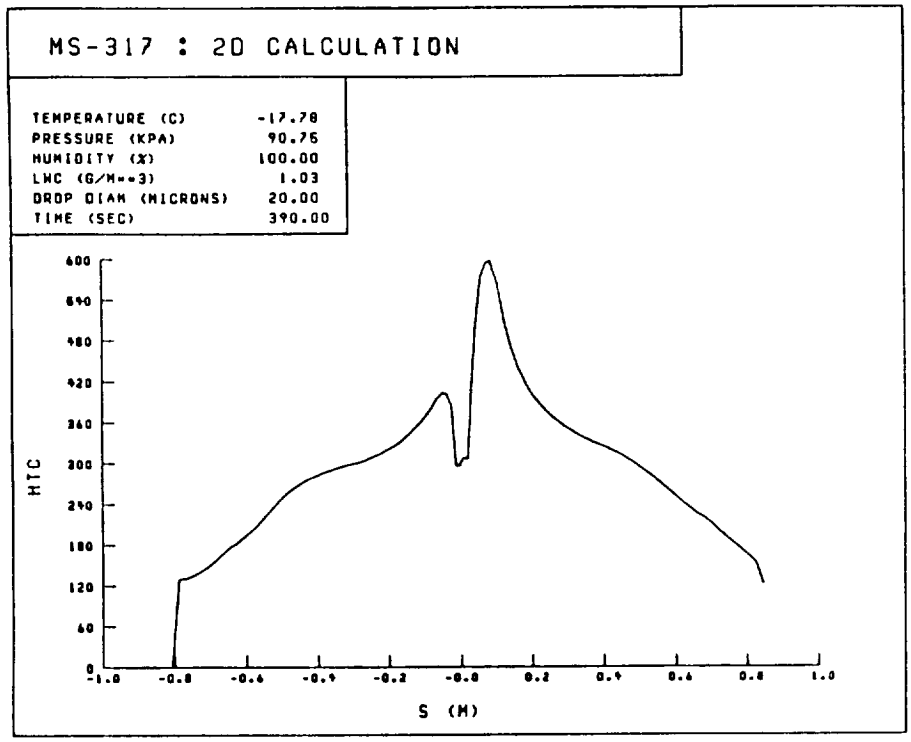

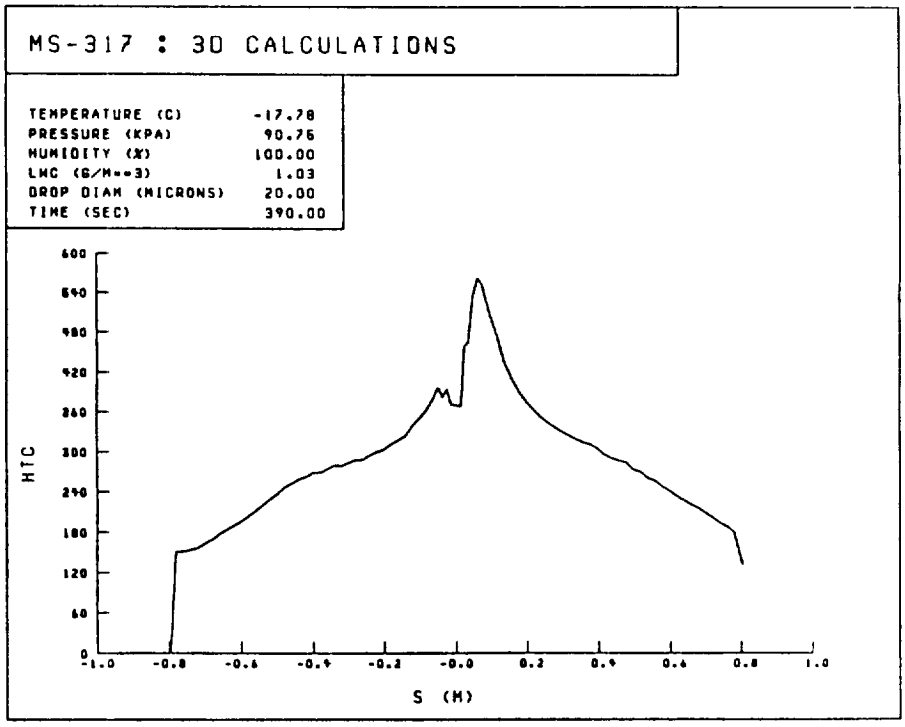

Figure 10. Convection Heat Transfer Coefficients in a Plane Normal to the Leading Edge for a MS-317 Swept Wing : 2D and 3D Calculations

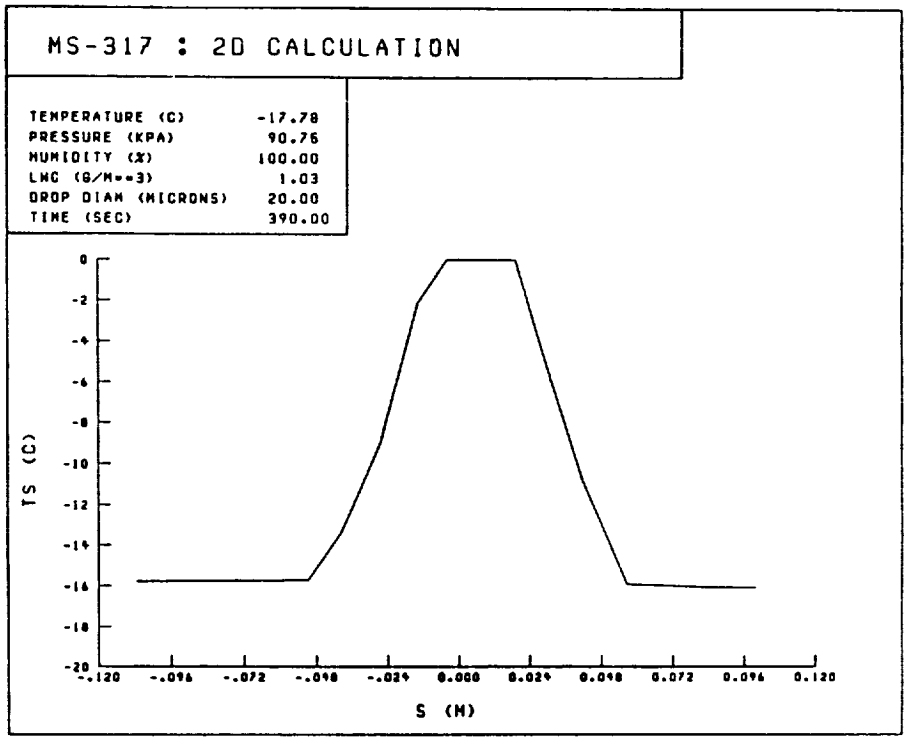

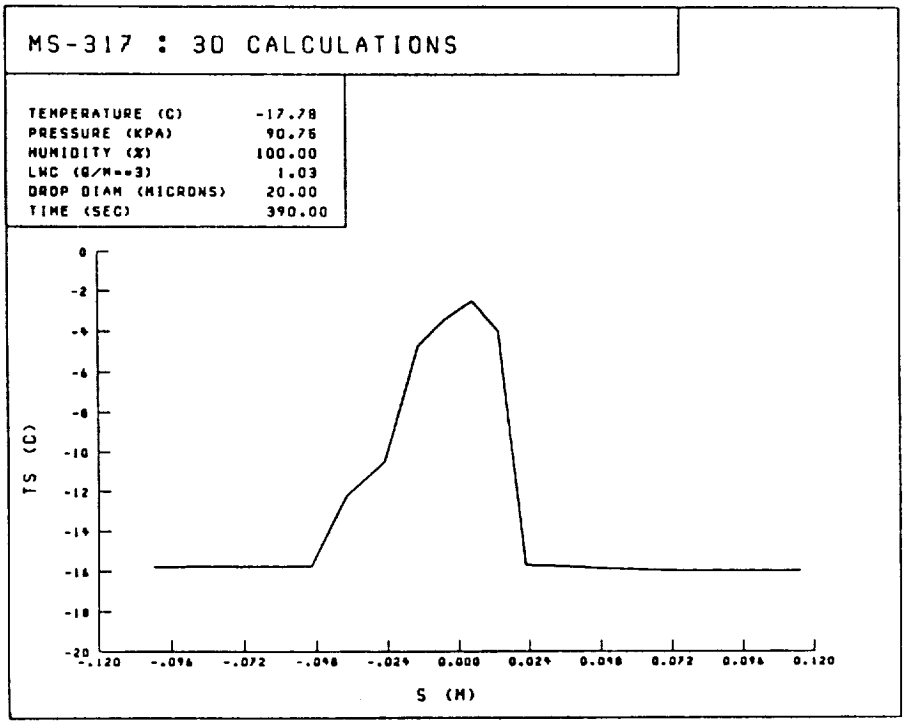

Figure 11. Surface Temperature Near Stagnation Region of MS-317 Swept Wing : 2D and 3D Calculations

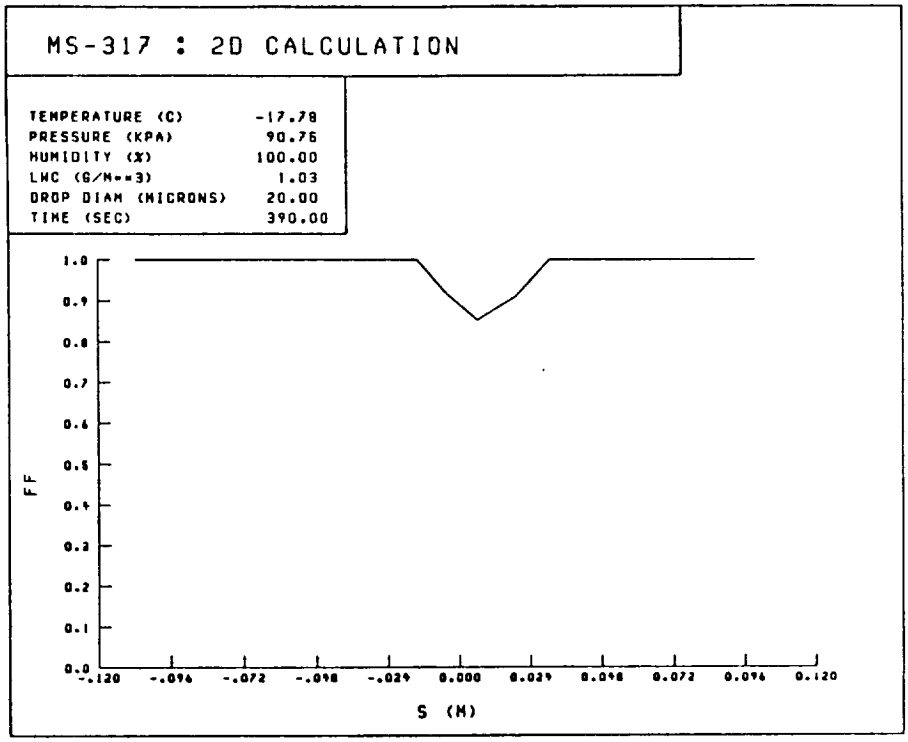

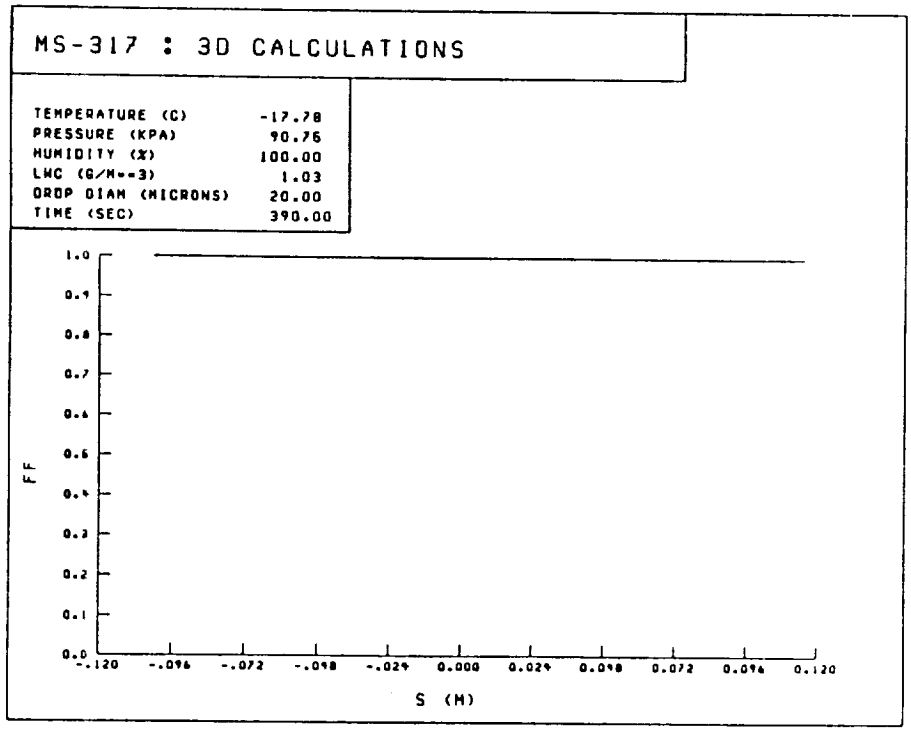

Figure 12. Freezing Fraction Near Stagnation Region of MS-317 Swept Wing ; 2D and 3D Calculations

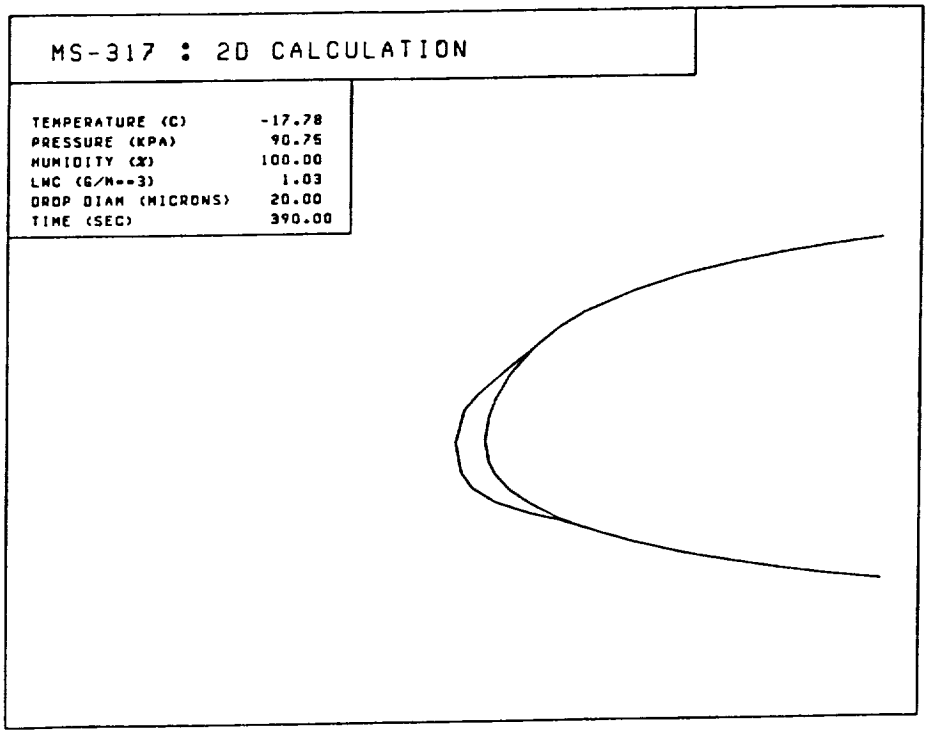

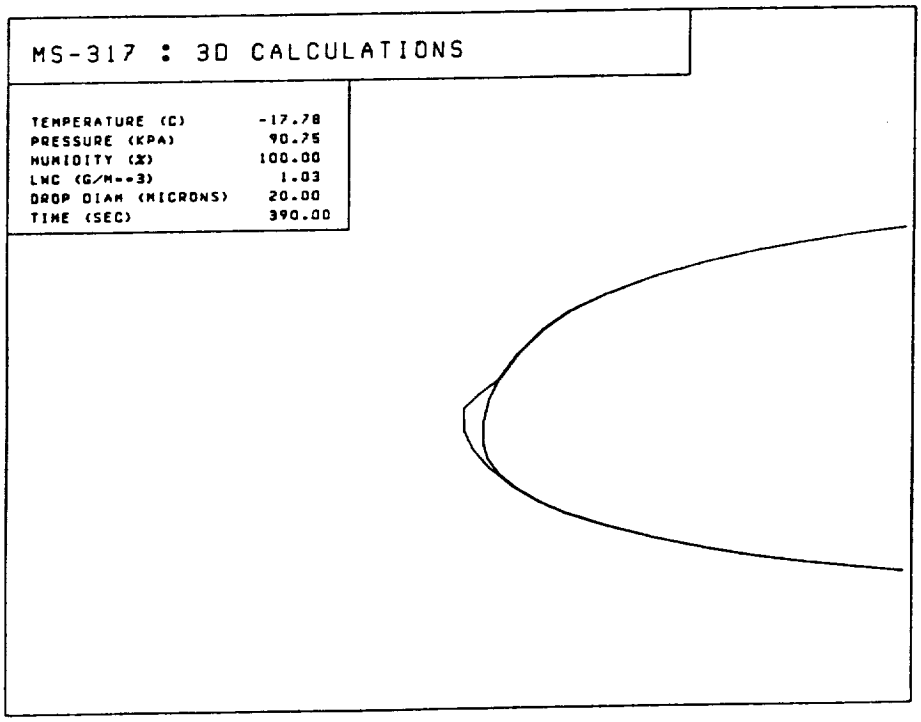

Figure 13. Ice Shape Profiles Near Leading Edge of MS-317 Swept Wing ; 2D and 3D Calculations

NASA
National Aeronautics and Space Administration

Report Documentation Page

1. Report No.	2. Government Accession No.	3. Recipient's Catalog No.
NASA TM-103114 AIAA-90-0756		

4. Title and Subtitle	5. Report Date
Swept Wing Ice Accretion Modeling	
	6. Performing Organization Code

7. Author(s)	8. Performing Organization Report No.
Mark G. Potapczuk and Colin S. Bidwell	E-5238
	10. Work Unit No. 505-68-11

9. Performing Organization Name and Address	11. Contract or Grant No.
National Aeronautics and Space Administration Lewis Research Center Cleveland, Ohio 44135-3191	
	13. Type of Report and Period Covered Technical Memorandum

12. Sponsoring Agency Name and Address	14. Sponsoring Agency Code
National Aeronautics and Space Administration Washington, D.C. 20546-0001	

15. Supplementary Notes

Prepared for the 28th Aerospace Sciences Meeting sponsored by the American Institute of Aeronautics and Astronautics, Reno, Nevada, January 8-11, 1990.

16. Abstract

An effort to develop a three-dimensional ice accretion modeling method has been initiated. This first step towards creation of a complete aircraft icing simulation code builds on previously developed methods for calculating three-dimensional flowfields and particle trajectories combined with a two-dimensional ice accretion calculation along coordinate locations corresponding to streamlines. This work is intended as a demonstration of the types of calculations necessary to predict a three-dimensional ice accretion. Results of calculations using the 3D method for a MS-317 swept wing geometry are projected onto a 2D plane normal to the wing leading edge and compared to 2D results for the same geometry. It is anticipated that many modifications will be made to this approach, however this effort will lay the groundwork for future modeling efforts. Results indicate that the flowfield over the surface and the particle trajectories differed for the two calculations. This led to lower collection efficiencies, convective heat transfer coefficients, freezing fractions, and ultimately ice accumulation for the 3D calculation.

17. Key Words (Suggested by Author(s))	18. Distribution Statement
Aircraft icing Computational fluid dynamics	Unclassified – Unlimited Subject Category 02

19. Security Classif. (of this report)	20. Security Classif. (of this page)	21. No. of pages	22. Price*
Unclassified	Unclassified		

NASA FORM 1626 OCT 86

*For sale by the National Technical Information Service, Springfield, Virginia 22161

ERRATA

NASA Technical Memorandum 103114

SWEPT WING ACCRETION MODELING

Mark G. Potapczuk and Colin S. Bidwell

Cover and Report Documentation Page: The NASA Technical Memorandum number should be changed from 102453 to 103114.